Research Article

Interfacing Sca-1pos Mesenchymal Stem Cells with Biocompatible Scaffolds with Different Chemical Composition and Geometry

G. Forte,[1,2] O. Franzese,[3] S. Pagliari,[1] F. Pagliari,[1] A. M. Di Francesco,[4] P. Cossa,[1] A. Laudisi,[3] R. Fiaccavento,[1,2] M. Minieri,[1,2] E. Bonmassar,[3] and P. Di Nardo[1,2]

[1] *Laboratorio di Cardiologia Molecolare e Cellulare, Dipartimento di Medicina Interna,*
 Università di Roma "Tor Vergata", 00133 Roma, Italy
[2] *Istituto Nazionale per le Ricerche Cardiovascolari (INRC), 40126 Bologna, Italy*
[3] *Dipartimento di Neuroscienze, Università di Roma "Tor Vergata", 00133 Roma, Italy*
[4] *Dipartimento di Oncologia Pediatrica, Policlinico Agostino Gemelli, Università Cattolica del Sacro Cuore, Roma, Italy*

Correspondence should be addressed to P. Di Nardo, dinardo@med.uniroma2.it

An immortalized murine mesenchymal stem cell line (mTERT-MSC) enriched for Lin[neg]/Sca-1pos fraction has been obtained through the transfection of MSC with murine TERT and single-cell isolation. Such cell line maintained the typical MSC self-renewal capacity and continuously expressed MSC phenotype. Moreover, mTERT-MSC retained the functional features of freshly isolated MSC in culture without evidence of senescence or spontaneous differentiation events. Thus, mTERT-MSC have been cultured onto PLA films, 30 and 100 μm PLA microbeads, and onto unpressed and pressed HYAFF-11 scaffolds. While the cells adhered preserving their morphology on PLA films, clusters of mTERT-MSC were detected on PLA beads and unpressed fibrous scaffolds. Finally, mTERT-MSC were not able to colonize the inner layers of pressed HYAFF-11. Nevertheless, such cell line displayed the ability to preserve Sca-1 expression and to retain multilineage potential when appropriately stimulated on all the scaffolds tested.

1. Introduction

Stem cells hold the potential to open up new and exciting perspectives to treat many degenerative diseases in the next future. Convincing evidences have been provided about the presence of multipotent progenitor cells within bone marrow and almost all organs [1], thus suggesting their implication in tissue homeostasis and their possible role as potential targets for innovative treatments. Therefore, the activation of resident stem cells in vivo by injecting growth factors or their administration into the damaged organs are currently investigated [2]. Alternatively, the engraftment of engineered tissue substitutes fabricated seeding stem cells on biodegradable, biocompatible scaffolds has been proposed as a more suitable solution to repair injured tissues [3, 4]. In fact, fine-tuned scaffolds could provide physical support to stem cell adhesion, proliferation, and differentiation, while favoring the organization of newly-formed tissues [5].

Natural (fibrin, chitosan, collagen, hyaluronic acid, . . .) and synthetic (poly-lactic and poly-lactic-co-glycolic acid, poly-caprolacton, . . .) compounds have been proposed as components of scaffolds for tissue engineering. Natural compounds better resemble the properties of extracellular matrix and are usually derived from animals, thus being potential vehicles for infectious diseases. Conversely, synthetic polymers can be more easily processed and sterilized before the implant and their degradation controlled [6]. Natural and synthetic materials are used to fabricate scaffolds with different structure and geometry (i.e., solid scaffolds, microbeads, hydrogels, foams, fibers, etc.), suitable for different applications. For example, fibrous scaffolds made of polycaprolactone (PCL) have been proposed for cartilage reconstruction [7], hyaluronan-based materials

for vasculogenesis [8], and alginate hydrogels for cardiac repair [9]. Additionally, biodegradable microbeads are under investigation to deliver cells and/or growth factors to treat neurodegenerative disorders [6].

The optimal combination of accurately designed scaffolds and autologous stem cells could represent an extraordinary chance to treat several degenerative diseases. In particular, the ability of bone marrow-derived mesenchymal stem cells (MSC) to generate virtually all cell lineages [10] in vitro as well as to engraft and home in vivo [11, 12] has raised great hope about their actual suitablity for clinical practice. Among the protocols so far adopted to purify MSC, the use of Stem Cell Antigen 1 (Sca-1) as a marker to enrich stem cells in a number of tissues is widely accepted [5, 13, 14]. In fact, Sca-1 expression has been associated to multipotency and self-renewal in bone marrow, skeletal muscles, dermis, heart, and liver [15]. However, Sca-1^{pos} mesenchymal stem cells isolated from murine bone marrow and cardiac stem cells from murine heart display multipotency in culture, but their differentiating potential on bidimensional and three-dimensional scaffolds made of synthetic polymers is not comparable. In fact, in our hands, bone marrow-derived MSC do not differentiate as a mere effect of scaffold physical factors, while cardiac stem cells in the same microenvironmental condition, express and assemble phenotype-specific proteins [5]. Therefore, the present study has been designed to challenge scaffolds with distinct chemical and structural composition and investigate their capability to affect Sca-1^{pos} MSC multilineage potential. On this purpose, polylactic acid (PLA) films and microbeads as well as two preparations of HYAFF-11, a hyaluronic acid derivative, have been utilized. However, in a preliminary step, since MSC undergo early senesce in vitro, an immortal line of murine Lin^{neg}/Sca-1^{pos} MSC has been generated through telomerase transfection and used to challenge scaffolds composed by different polymers and displaying distinct structure. This demonstrated that Sca-1 antigen, although identified as a stemness marker, does not concur to regulate stem cell lifespan in culture, while confirming that the ectopic expression of telomerase reverse transcriptase (TERT), the *catalytic subunit of telomerase*, has the ability to extend MSC lifespan preserving stemness features [16–18].

2. Materials and Methods

2.1. Isolation and Culture of Murine Lin^{neg} Sca-1^{pos} MSC. Lineage negative, Sca-1 positive mesenchymal stem cells (Lin^{neg}/Sca-1^{pos} MSC) were obtained from 6-week-old female C57/Bl mice femurs by 2 sets of magnetic cell sorting protocol (Miltenyi Biotec GmbH, Bergisch Gladbach, Germany), as described elsewhere [5]. An aliquot of each separated cell subpopulation (Lin^{neg}/Sca-1^{pos} and Lin^{neg}/Sca-1^{neg}) was then stained with anti-Biotin PE-conjugated secondary antibody and analyzed with fluorescence activated cell sorter. The Lin^{neg}/Sca-1^{pos} fraction was resuspended in complete IMDM medium (Iscove's Modified Dulbecco medium, Cambrex Bio Science, Verviers, Belgium) sup-

plemented with 10% FCS, 1× ITS, 100 IU/mL penicillin and 10 μg/mL streptomycin. This medium will be hereafter referred to as complete medium.

2.2. Construction of a Vector Expressing mTERT. To produce a vector expressing mTERT, pcINeo plasmid (Promega, Madison, Wis, USA) was digested with EcoRI and the mTERT coding sequence, obtained from plasmid pGRN190 (a kind gift from Geron Corporation), was inserted into the same restriction site EcoRI. The resulting transfer plasmid was named pCINeo-mTERT.

2.3. Transfection with pCINeo-mTERT. For transfection experiments, 10 μg of plasmid pCINeo-TERT or control vector pCINeo were introduced into p10 Lin^{neg}/Sca-1^{pos} MSC cells using the Calcium Phosphate Method (Promega, Madison, Wis, USA), according to manufacturer instructions.

Passage 10 (p10) Lin^{neg}/Sca-1^{pos} MSC were plated at 50% confluence on day 0 and medium was changed on day 1, 4 hours before transfection. After transfection (12–16 hours), the calcium-phosphate containing medium was removed and cells were washed and incubated with fresh medium.

2.4. Single-Cell Clone Isolation. To obtain single-cell clones, mTERT-MSC were plated into 96-well plate at a single-cell level by limiting-dilution method and cultured with conditioned medium. To obtain conditioned medium, mTERT-MSC supernatant was filtered through a 0.22 μm sterile filter and diluted 1 : 1 with fresh medium. Wells were inspected under light microscopy every day to exclude those containing more than 1 cell. Clones derived from a single cell were further cultured to 70–80% confluence and seeded into 1 well of a 24-well plate and thereafter serially reseeded in 6-well dishes, 25-cm^2, and 75-cm^2 flasks.

2.5. Measurement of Telomerase Activity. Telomerase activity was determined according to the telomeric repeat amplification protocol (TRAP). Briefly, telomerase activity was assayed in whole cell extracts. Cell samples for detection of telomerase activity were collected at the times indicated in the results. Cells were washed in PBS and lysed in ice-cold extraction buffer containing 0.5% 3[(cholamidopropyl)-dimethyl-ammonium]-1-propanesulfonate, 10 mM Tris-HCl (pH 7.5), 1 mM MgCl$_2$, 1 mM EGTA, 5 mM β-mercaptoethanol, 0.1 mM [4(2-aminoethyl)-benzenesulfonyl fluoride] hydrochloride, and 10% Glycerol (SIGMA-ALDRICH, Milano, Italy). Extracts obtained from 5×10^3 cells were used for TRAP assay. TRAP assay was performed in 50 μL of reaction mixture [20 mM Tris-HCl (pH 8.3), 68 mM KCl, 1.5 mM MgCl$_2$, 1 mM EGTA, 0.05% Tween 20, 0.1 μg of TS (AATCCGTC-GAGCAGAGTT) primer, 0.5 mM T4 gene 32 protein, 10 mM deoxynucleotide triphosphate, 2 units of Taq polymerase (Promega, Madison, Wis, USA), and 2 μCi of (α-^{32}P)-dCTP (3000 CI/mmol; DuPont NEN Research Products, Boston, Mass, USA)]. Each reaction was carried out in a single PCR tube containing 100 ng of CX oligonucleotide (CCCTTTA)

TABLE 1: Primers used in the study.

	Forward	Reverse
Islet-1	5'-GCCTCAGTCCCAGAGTCATC-3'	5'-AGAGCCTGGTCCTCCTTCTG-3'
Nestin	5'-TCAAGGGGAGGCCAGGAAGGA-3'	5'-CTGCAGCCCCACTCAAGCCATC-3'
Nucleostemin (NST)	5'-GGGAAAAGCAGTGTCATTA-3'	5'-GGGATGGCAATAGTAACC-3'
Nanog	5'-ATGGTCTGATTCAGAAGGGC-3'	5'-TTCACCTTCAAATCACTGGC-3'
GAPDH	5'-CAAGATGGTGAAGGTCGGTGTG-3'	5'-GGGGTAAGCAGTTGTGTCAGGAT-3'

3CCCTAA (Biogen, Rome, Italy) sealed at the bottom of the tube by a wax barrier. Samples were incubated at 22°C for 20 minutes to allow telomerase to extend TS primer, followed by a 31-cycle PCR amplification (Perkin Elmer Corp., Norwalk, Conn, USA) of the telomeric products. An internal control (IC) was included in the reaction mixture. Forty μL of PCR products were run on 10% nondenaturing Acrylamide gels. Gels were fixed in 0.5 M NaCl, 50% Ethanol, and 40 mM Sodium Acetate (pH 4.2) and then exposed to X-Ray Film (Kodak, Rochester, NY, USA). Band intensity was quantified by bidimensional densitometry, using a Bio-Rad scanning apparatus (Bio-Rad Imaging Densitometer, GS-670; Molecular Analyst Software, Richmond, Calif, USA).

2.6. Measurement of Population Doublings. Cells were seeded at the concentration of $2 \times 10^4/cm^2$ in correspondence of each passage. Cell viability was quantified by Trypan blue exclusion every second day. The assessment of proliferative capacity was performed by calculating the number of population doublings, using the formula $\log_{10}$(total no./start no.)/$\log_{10} 2$.

2.7. MSC Differentiation Protocols. mTERT-MSC, passage 1 (p1) and passage 10 (p10) MSC were plated onto 35 mm dishes (2×10^5 cells/dish) or onto the scaffolds and cultured in adipogenic or osteogenic medium (Cambrex Bio Science, Verviers, Belgium). The medium was changed every second day. Adipored (Cambrex Bio Science, Verviers, Belgium) or Alizarin Red S staining was used to assess the occurrence of adipogenic or osteoblastic differentiation after 10 days. Cells cultured in absence of induction mediums were used as negative controls. The presence of lipid vacuoles was visualized under fluorescence microscope, while the production of calcium deposits was confirmed in light microscopy.

2.8. RNA Extraction, Retrotranscription, and Semiquantitative PCR. Total RNA was extracted by Trizol Reagent (GIBCO BRL, Gaithersburg, Md, USA). Retrotranscription was carried out with 2 μg of RNA for each sample using RT M-MLV (Invitrogen, Calif, USA) in the presence of random hexamers. Semiquantitative analysis of RNA expression was carried out by RT–PCR by comparing the control transcript (GAPDH) and the transcript of interest when their amplification was in the exponential phase. Total DNA was then extracted from the interphase and phenol phase according to manufacturer instruction. The primers used are reported in Table 1. PCR products were size-fractionated in 2% agarose gel electrophoresis.

2.9. FACS Analysis. To analyze Annexin V expression, cells were treated according to the manufacturer instruction (SIGMA-ALDRICH, Milano, Italy). For intracellular protein staining, cells were fixed and permealized using the Intraprep TM kit (Beckman Coulter), following manufacturer instruction, and incubated for 30 minutes with anti-Sca-1-PE antibody (PharMingen, Calif, USA) or CD105, FLK1, CD90, CD31, MDR-1 (Santa Cruz Biotechnology, Calif, USA), washed with ice-cold PBS and incubated 30 min with FITC-conjugated secondary antibody (Vector Laboratories, Ltd, Peterborough, UK). After incubation, cells were washed with ice-cold PBS and analyzed in a FACScalibur flow cytometer (BD PharMingen, Calif, USA).

2.10. Immunofluorescence. Passage 1, passage 10 MSC and mTERT-MSC were seeded at the concentration of $2 \times 10^4/cm^2$ on chamber slides (Nalgene, Nunc, Thermo Scientific, NY, USA). Cells were washed in PBS, fixed in paraformaldehyde (PFA) 4% in PBS containing $CaCl_2$ for 30 minutes at 4°C and permeabilized with 0.1% Triton X-100. Cells were stained with Tetrarhodamine-conjugated Phalloidin, directed against F-actin (Invitrogen Corp., Calif, USA), Nuclei were stained with $4',6'$-diamidino-2-phenylindole (DAPI, Invitrogen, Calif, USA). The images were taken using a Leica DMRB microscope equipped with a digital camera.

2.11. Western Blot Analysis. For total cellular extraction, cells were washed twice with ice-cold (PBS phosphate-buffered saline), detached with Trypsin/EDTA solution and lysed in RIPA buffer (150 mM NaCl, 50 mM Tris-HCl [pH 7.4], 1% Nonidet P-40, 0.25% sodium deoxycholate, 2 mM ortho-vanadate and a cocktail of protease inhibitors (SIGMA-ALDRICH, Milano, Italy). Cell lysates were centrifuged at 13000 rpm at 4°C for 15 minutes, protein content quantified by Bradford method (Amresco, Inc., Fla, USA), and extracts (50 μg) resolved on sodium dodecylsulfate–12,5% polyacrilamide gel electrophoresis (SDS-PAGE), followed by transfer onto PVDF filters. Filters were blocked with PBS/milk 7% and protein analysis carried out using the following primary antibodies: polyclonal Abs against TERT (Calbiochem, CA, USA), against. Protein expression was detected with horseradish-peroxidase conjugated appropriate secondary antibodies followed by enhanced chemiluminescence reaction (ECL, Amersham Plc, UK). Cytosol and
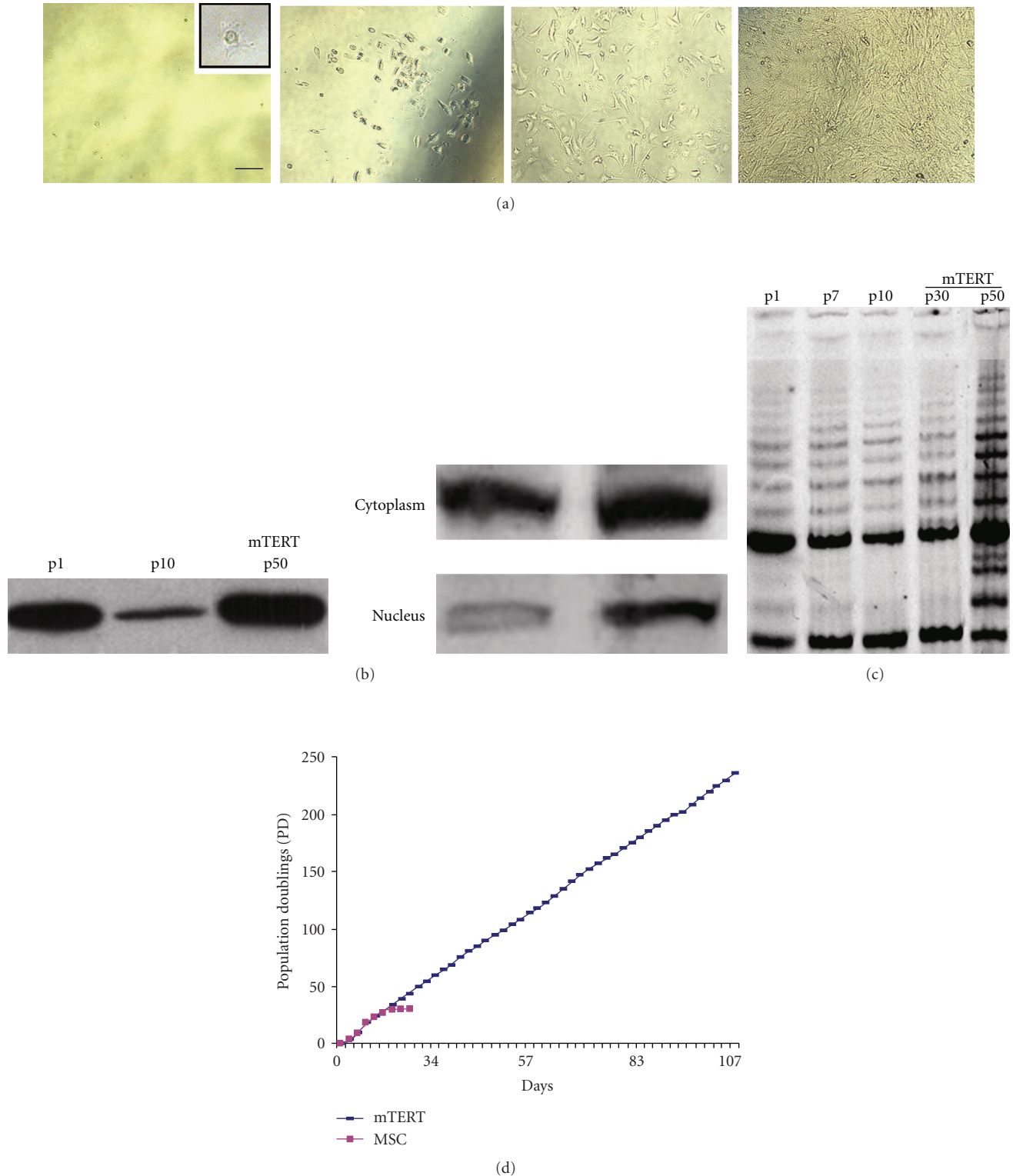
(a)

(b)

(c)

(d)

FIGURE 1: *Generation of mTERT-MSC cell line*. (a) Single cell cloning (limiting dilution) of mTERT-MSC cell line. Following cell transfection and G418 selection, single cell cloning was adopted to obtain a purified Sca-1^{pos} mTERT-MSC. Different time points along the culture are shown (bar: 50 μm). (b) Western blot analysis of mTERT protein expression tested on extracts from mTERT-MSC and control cells at different culture time points (p1, p10), and nuclear localization of mTERT protein; (c) Telomerase activity (TRAP Assay) of Sca-1^{pos} MSC transduced with mTERT, compared to controls, evaluated at different culture time points. Telomerase activity was tested on extracts corresponding to viable 5×10^3 cells. The pattern of TRAP reaction represents a ladder of bands with a periodicity corresponding to multiples of TTAGGG telomeric repeats. Band intensity was quantified by bi-dimensional densitometry; (d) comparison between MSC and mTERT-MSC proliferation, expressed as population doublings (PD), determined as described in Section 2.

nuclear extracts were prepared as previously described [17]. Cellular proteins from 5×10^6 viable cells were separated by 10% SDS–PAGE, transferred to Hybond-P membranes (Amersham Pharmacia Biotech, Piscataway, NJ, USA). Filters were probed as described above.

2.12. FLARE (Fragment Length Analysis using Repair Enzymes) Comet Assay . Briefly, control and mTERT transduced cells were treated with increasing concentrations of H_2O_2 and incubated at 37°C, 4 hours. Then, after H_2O_2 wash-out, cells were embedded in 1% low melting point agarose and poured onto agarose precoated glass slides. Gels were allowed to set on a cold plate, then slides were immersed in cold lysis solution (2.5 M NaCl, 100 mM Na$_2$EDTA, 10 mM Tris Buffer, pH 10.5; 1% DMSO, and 1% Triton X-100, added just before lysis) for 1 hour at 4°C in the dark. Following lysis, slides were first washed in distilled water (four washings of 5 min each) and then immersed in two changes of buffer F [40 mM HEPES, 0.1 M KCl, 0.5 mM EDTA and 0.2 mg/ml BSA (pH 8)] for 5 minutes, each time at room temperature. hOOG1 (New England BioLabs, Mass, USA) was then added to each gel in $70 \mu L$ buffer F at a dilution (1 : 500) previously shown by titration to give the highest percentage of breaks following H_2O_2 treatment. Gels were covered with a cover slip and incubated in a humidified chamber for 45 min at 37°C. Then cover slips were removed and slides were placed on an electrophoretic platform covered with electrophoresis buffer [1 mM Na$_2$EDTA, 0.3 M NaOH, pH > 13] where the DNA was allowed to unwind for 20 minutes before electrophoresis at 0.7 V/cm, 300 mA for further 20 minutes at 4°C. Slides were then removed and immersed in three changes of neutralizing buffer [0.4 M Tris-HCl (pH 7.5)] for 5 minutes at room temperature, then stained with Sybr Gold [1 : 10000 solution in alkaline water, pH 8 (Bioproducts, Rockland, USA)] and scored 5 minutes later. For each sample, 100 cells (50 per duplicate slide) were acquired using a Zeiss fluorescence microscope connected to a Ultrak CCD black and white camera. Statistical calculations of the %Tail DNA were carried out using the Kinetic Komet 5.0 software from Kinetic Imaging Ltd. (Liverpool, UK).

2.13. Cell Culture and Analysis on Substrates. For poly-lactic acid (PLA, Lactel Absorbable Polymers, Cupertino, CA, http://www.absorbables.com/) film fabrication, the polymer was diluted in methylene chloride (SIGMA-ALDRICH, Milano, Italy) and then spincoated onto glass coverslips (2 mm diameter) by applying 0.5 mL of 20% solution and spinning at 400 rpm (SUSS Microtech, Zurich, Switzerland, http://www.suss.com/) to obtain thin films of approximately $380 \mu m$-height, as assessed by SEM analysis (data not shown). Two forms of hyaluronan total benzyl ester (HYAFF-11, Fidia Advanced Biomaterials, Italy) nonwoven scaffolds were used: unpressed and pressed felts. The two formulations of HYAFF-11 show rather different macroscopic aspect, as a result of their composition: mean diameter of the fibers in the unpressed scaffolds ranges between $10–30 \mu m$, while fibers in pressed felts have 500–600 nm diameter (SEM analysis, data not shown). PLA microbeads with 30 or $100 \mu m$ diameter were purchased from Corpuscular Inc (NY, USA). All the scaffolds were washed twice with 70% ethanol and sterilized under UV light for 15 minutes. Two mg of microbead preparation were centrifuged at 14000 rpm for 5 minutes and resuspended in complete medium. Afterwards, all the scaffolds were incubated for 4 hours with complete medium at 37°C. Therefore, the medium was gently removed and mTERT-MSC seeded onto the scaffolds. The cells were seeded at the concentration of 5×10^5/well on the microbeads, at 5×10^5/cm^2 onto PLA films and HYAFF scaffolds in low attachment wells (Corning Life Sciences, Mass, USA).

3. Results

3.1. Generation of Immortalized Sca-1^{pos} MSC Cell Line. Lin^{neg}/Sca-1^{pos} MSC were obtained by two subsequent sets of immunopurification of adherent bone marrow progenitors by anti-Lin-cocktail and- Sca-1+ antibodies (Miltenyi Biotec GmbH, Germany). Cells were cultured until the 10 th passage and then transfected with either pCINeo-mTERT expression or control vector pCINeo by Calcium Phosphate, as described in Section 2. Cells overexpressing mTERT were selected with G418, at the concentration of $300 \mu g$/ml for 2 weeks. Single cell-derived colonies were isolated by limiting dilution and cultured in complete medium (Figure 1(a)). Telomerase ectopic transduction resulted in the accumulation of mTERT protein in transfected MSC (Figure 1(b)). As expected, mTERT-MSC showed increased levels of mTERT protein in the nuclear compartment, as compared to passage 1 MSC (Figure 1(b), right panel). Moreover, a progressive upregulation of functionally active telomerase (Figure 1(c)) was detected in mTERT-MSC (at p30 and p50), in TRAP assay, as compared to control cells at passages 1 (p1), 7 (p7), and 10 (p10). Cell proliferative capacity was assessed calculating the number of population doublings, using the formula $\log_{10}$(total no./start no.)/$\log_{10}$2. While control MSC underwent 30 population doublings before exiting proliferation and proceeding to senescence, mTERT-transduced cells showed a significant up-regulation in the number of population doublings (more than 300, Figure 1(d)), and are still in culture.

3.2. mTERT-MSC Retain Morphology, Phenotype, and Functional Features of Freshly Extracted Sca-1^{pos} MSC. Proliferating undifferentiated MSC displayed typical fibroblastoid morphology and grew in a monolayer until confluence (Figure 2(a)), while they became senescent after 10–12 passages in culture, showing flattened morphology (Figure 2(b)). After the transfection, mTERT-MSC displayed the typical elongated morphology and the capacity to grow in a monolayer (Figure 2(c) and inset for higher magnification). Moreover, semiquantitative RT-PCR and FACS analyses demonstrated that no significant difference was detectable in stemness marker expression (Sca-1, Islet-1, Nst, Nanog and Nestin, CD105) as compared to p1 and p10 MSC (Figures 2(d) and 2(e)). A thorough characterization of mTERT-MSC
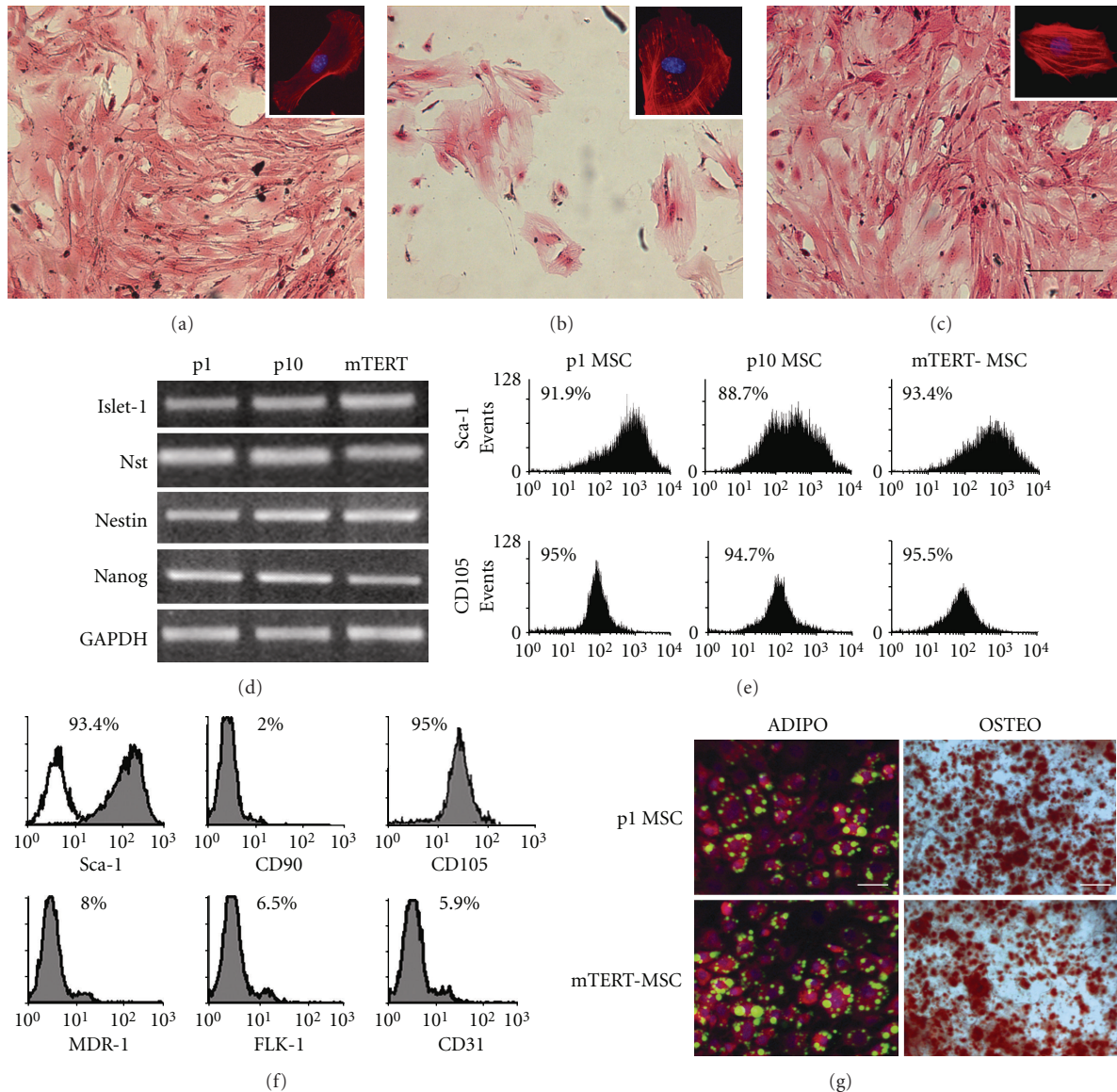
(a)

(b)

(c)

(d)

(e)

(f)

(g)

FIGURE 2: *mTERT-MSC line retains morphology, phenotype, and multilineage capacity of Sca-1^{pos} MSC.* (a) Freshly extracted (p1) Sca-1^{pos} MSC show typical spindle-shaped morphology (see inset), while (b) after 10 passages in culture they proceed to senescence and fail to grow as monolayer; (c) mTERT-MSC preserve the ability to grow in a monolayer. Bar; 20 μm; (d, e) semiquantitative RT-PCR and FACS analyses showing that mTERT ectopic expression preserves typical Sca-1^{pos} MSC stem cell phenotype; (f) thorough characterization of mTERT-MSC phenotype; (g) comparison between mTERT-MSC and MSC multilineage potential in culture (Bars: 100 μm).

line demonstrated that they expressed high levels of Sca-1, CD105, and low levels of MDR-1, CD90, FLK-1, and CD31 (**Figure 2(f)**). Finally, mTERT-MSC preserved multipotential capacity, as compared to freshly extracted (passage 1) MSC (**Figure 2(g)**). These features were retained for more than 150 passages in the same culture conditions (data not shown).

3.3. mTERT Transduction Protects MSC from H_2O_2-Induced Apoptosis. Preliminary experiments showed that micromolar concentrations of H_2O_2 did not induce a significant increase in the number of MSC apoptotic cells (data not shown). Therefore, only 5 μM H_2O_2 was included in this set

of experiments. Higher H_2O_2 concentrations were able to induce apoptosis in control cells, while mTERT overexpression prevented this effect in MSC (**Figure 3(a)**). Therefore, the ability of mTERT to protect MSC from apoptosis following H_2O_2-induced oxidative stress was investigated. Control and mTERT-MSC were challenged with increasing concentrations of H_2O_2 (ranging from 5 μM to 50 mM) for 4 hours and early apoptosis assessed by cytofluorimetric analysis of the percentage of Annexin V positive cells. The analysis of basal cell apoptosis showed that no significant differences were detectable in mTERT-transduced cells versus control cells (p1 MSC), indicating that mTERT overexpression was not able to confer resistance to spontaneous apoptosis
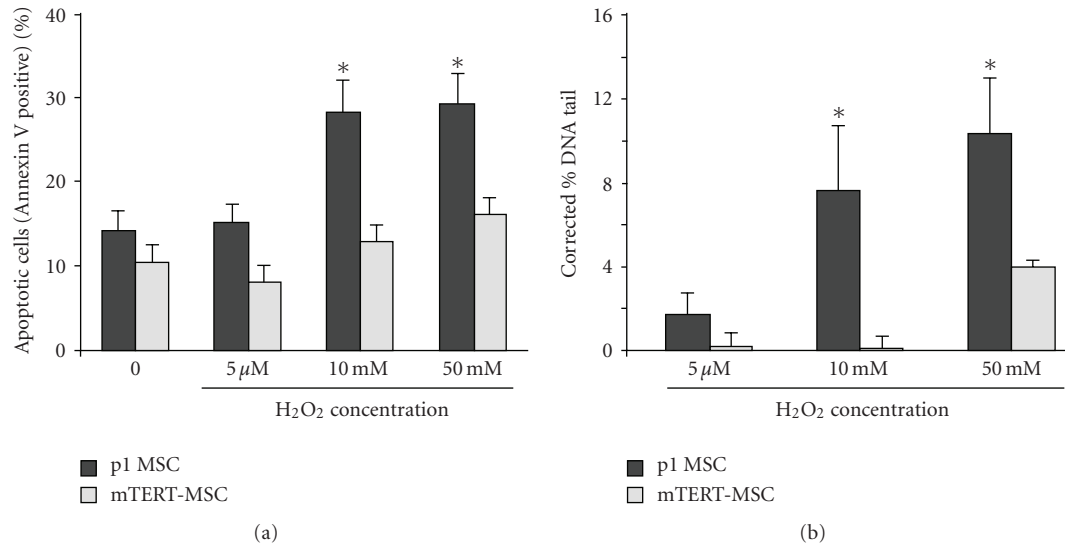
(a)

(b)

FIGURE 3: *mTERT protects Sca-1*^{pos} *MSC from oxidative stress induced by high concentrations of* H_2O_2. (a) mTERT-MSC show lower susceptibility to apoptosis induced by high H_2O_2 concentrations. DNA damage measured as the mean Comet %Tail DNA of control MSC and mTERT-MSC cells treated with high H_2O_2 concentrations. Untreated cells were used as negative controls (no damage). The results obtained for the enzyme treatment (hOGG1) were normalized by subtracting the level of %Tail DNA observed with the enzyme-buffer only. The number of cells scored for each sample was 50 and the data are a mean of two experiments. Error bars denote S.E. *$P < .005$, MSC versus mTERT-MSC.

(Figure 3(a)). Conversely, apoptosis in MSC overexpressing mTERT was significantly reduced after challenging cells with H_2O_2 concentrations $>5\,\mu M$, as compared to control cells. The oxidative DNA damage caused by reactive oxidative species (ROS) can be detected by evaluating the levels of 8-oxo-7,8-dihydro-2′-deoxyguanosines (8-oxodG) [18]. In this study, (FLARE Fragment Length Analysis using Repair Enzymes)—Comet assay, a modified version of the alkaline comet assay (single-cell gel electrophoresis), was used to detect and measure the H_2O_2-induced oxidative damage in control and mTERT-transduced MSC. DNA damage was measured as the mean Comet % tail of control MSC at passage 1 (p1 MSC) and p50 mTERT-MSC cells treated with increasing concentrations of H_2O_2. The overexpression of mTERT was able to protect MSC from DNA damage induced by H_2O_2 at all concentrations tested (Figure 3(b)). Similar results were obtained using mTERT-MSC in correspondence of later passages (data not shown).

3.4. mTERT-MSC Behavior onto Injectable and Fibrous Scaffold of Biodegradable, Biocompatible Polymers. mTERT-MSC line was used to test the possibility that different scaffolds could sustain stem cell adeshion, growth, and differentiation. On this purpose, p68 mTERT-MSC were seeded onto PLA films and microbeads (30 and 100 micron diameter) and onto pressed and unpressed HYAFF-11 felts. Cell adhesion was studied after 2, 4, and 6 days by hematoxylin-eosin staining. As shown in Figure 4(a), the cells were able to adhere to all the surfaces tested. Nevertheless, some significant differences were detectable: clusters of mTERT-MSC were found on PLA microbeads after 4 and 6 days. Moreover, the

cells were not able to colonize the inner layers of pressed HYAFF-11 and formed a monolayer (but many aggregates wrapped single fibers at the end of the scaffold) which detached after 2 days. On the contrary, cells were found in the core of unpressed HYAFF-11 felts. Figure 4(b) shows that no significant differences in Sca-1 expression was detected after 6 days on all the matrices considered.

This result was strengthened by the evidence that after 2 weeks on all the scaffolds tested, mTERT-MSC still retained multilineage capacity, as shown in Figure 5.

4. Discussion

The complex relationship between stem cells and polymeric scaffolds has been analyzed in few studies, so far [5, 19–21]. Scaffold chemistry, geometry, and manufacturing process play a pivotal role in directing Sca-1^{pos} cardiac resident stem cell (CSC) commitment towards the cardiac phenotype. However, scaffold properties exert different effects on distinct stem cell populations; in fact, bone marrow-derived mesenchymal stem cells (MSC) do not activate the same gene programs as CSC, when cultured in the same conditions (scaffold/culture medium) thus suggesting that MSC and CSC do not share all their functional features, the latter being more prone to acquire the cardiac phenotype when challenged by an adequate microenvironment [5].

The present study was designed to give an insight in Sca-1^{pos} MSC ability to retain their own multilineage potential when cultured on scaffolds with different chemical and physical properties. Unfortunately, cultured MSC proceed to senescence within few passages [22], indicating that the
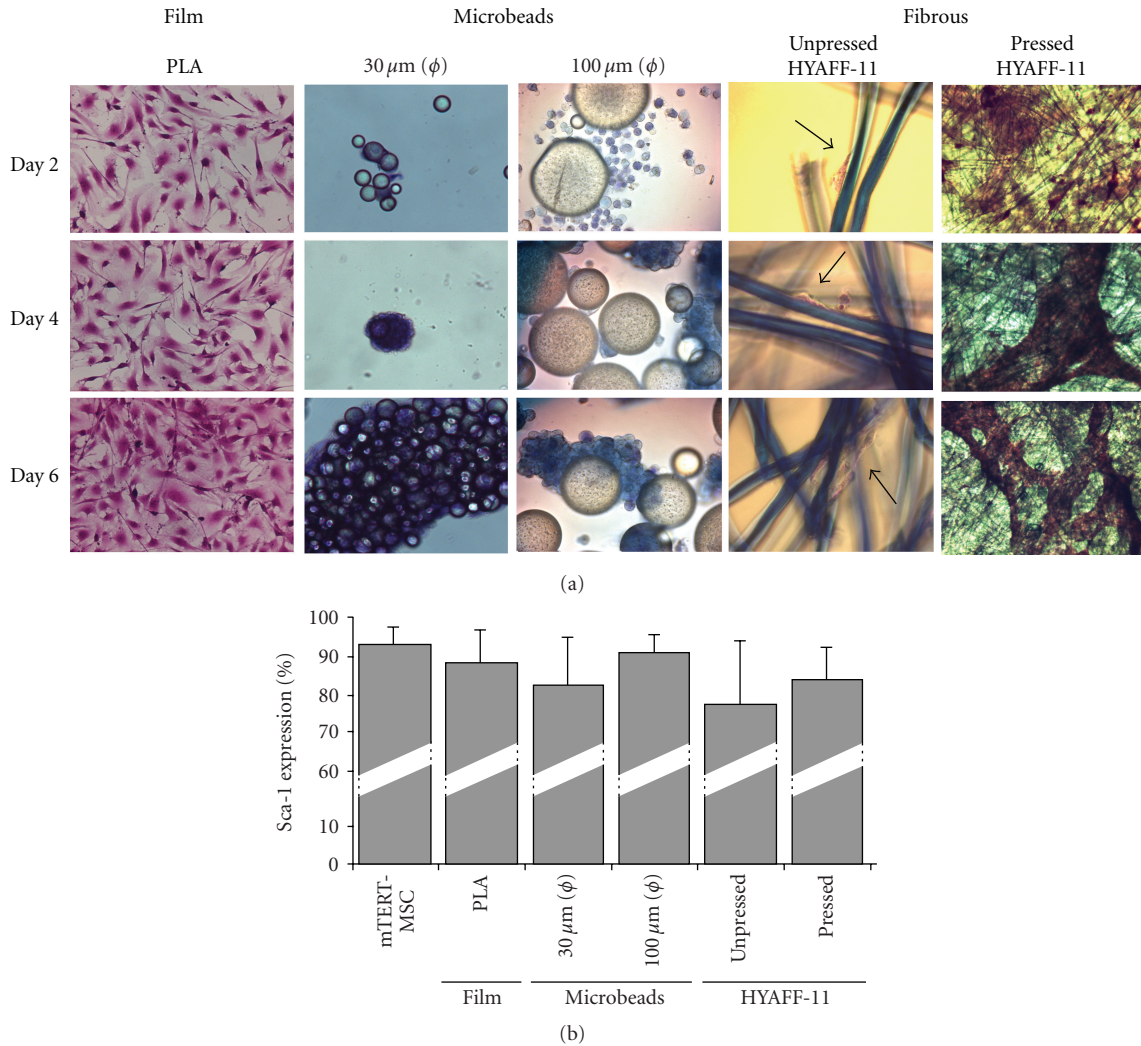
(a)

(b)

FIGURE 4: *mTERT-MSC cell line preserves Sca-1 expression on different biocompatible scaffolds.* (a) Hematoxylin/eosin staining of mTERT-MSC grown on PLA films, 30 μm, 100 μm diameter microbeads, unpressed and pressed HYAFF-11 felts, after 2, 4, and 6 days in culture. (b) No significant differences in Sca-1 expression was detected in mTERT-MSC grown on the scaffolds. The results are expressed as the mean of 3 experiments, ±SEM.

expression of Sca-1 antigen, which has been associated with self- renewal and multilineage potential in stem cell populations from virtually all the organs [15], is not sufficient to extend MSC lifespan in culture. For this reason, in a first step of the present investigation, a novel purified murine Sca-1^{pos} mesenchymal stem cell line (dubbed mTERT-MSC) has been generated by transfecting purified Sca-1^{pos} mesenchymal progenitors isolated from the murine bone marrow with the catalytic subunit of telomerase enzyme mtert. This procedure has already been proven effective in extending lifespan in embryonic [23] and adult stem cells [24–26]. Here, we confirm that the transfection of Sca-1^{pos} MSC with mTERT results in the generation of an MSC cell line (mTERT-MSC) permanently displaying undifferentiated morphology and phenotype, as well as multipotential ability, which are typical hallmarks of freshly isolated mesenchymal stem cells [10, 27]. mTERT-transduced Sca-1^{pos} MSC showed upregulation

of mTERT protein levels in the nuclear compartment, as compared to untransfected controls. This observation suggested that ectopic mTERT underwent the process of phosphorylation and activation by cell kinases [28], which allows its translocation to the nuclear compartment [29].

mTERT-MSC line behaved exactly like native, freshly isolated MSC and, thus, could be used as a suitable model to study mesenchymal stem cell culture onto a series of scaffolds, which have already proven effective in vitro [5, 8, 28] and are under evaluation for clinical applications. On this purpose, PLA films and microbeads, altogether with two different preparations of hyaluronan-based scaffolds have been challenged for their capacity to sustain mTERT-MSC adhesion, growth, and multilineage differentiation. The scaffolds used in the present study were chosen since they are representative of almost all classes of synthetic and natural matrices (injectable, solid, and fibrous) available

| | Film | Microbeads | | Fibrous | |
| | PLA | 30 μm (ϕ) | 100 μm (ϕ) | Unpressed HYAFF-11 | Pressed HYAFF-11 |

ADIPO

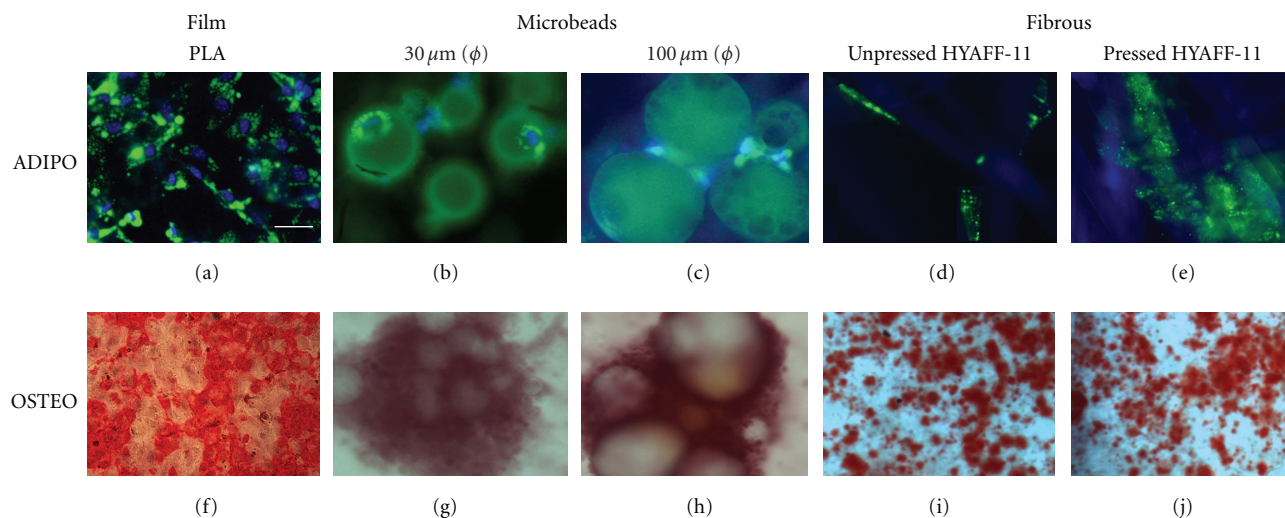(a)　　　　(b)　　　　(c)　　　　(d)　　　　(e)

OSTEO

(f)　　　　(g)　　　　(h)　　　　(i)　　　　(j)

FIGURE 5: *mTERT-MSC cell line displays multilineage differentiation on different biocompatible scaffolds.* Adipogenic (a)–(e) and osteogenic (f)–(i) differentiation of mTERT-MSC on the scaffolds. The occurrence of adipogenesis was assessed by ADIPORED staining (green: lipid droplets; blue DAPI: nuclei), while calcium deposits are decorated with ALIZARIN RED S.

for tissue engineering. All the scaffolds used in the present study allowed mTERT-MSC adhesion without evidence of toxic effects, as demonstrated by the absence of floating cells within the well during the culture (data not shown). Nevertheless, in vivo experiments demonstrated that PLA scaffold degradation can cause local pH alteration and limited immune response. On the contrary, hyaluronic acid degradation does not produce any adverse by-products, but can be vehicles for infectious diseases [8]. Interestingly, some clear differences in cell behavior on the matrices were noticed. As expected, cell distribution onto PLA films was uniform, with cells retaining their spindle-shaped morphology. On the contrary, cell adhesion onto PLA beads resulted in the formation of cell clusters, which made difficult any further quantitative analysis or longer culture. Notably, mTERT-MSC were able to migrate through the unpressed scaffolds and colonize the inner layers, whereas cells did not penetrate the surface of the pressed scaffolds. This phenomenon, already observed when using endothelial cells, has been explained suggesting that larger pores and an open structure favour cell migration within the scaffold [8]. In the present study, a significant difference was found in the diameter of fibers in pressed versus unpressed HYAFF-11 formulations, the former having nanoscale width, the latter showing fibers in the microscale range. The tight stacking of nanofiber network in pressed scaffolds could indeed represent an obstacle for cell colonization, as previously proposed [30]. Such evidence appears of great interest since the unpressed felts could be useful to obtain thick tissue-substitutes, while the pressed ones appear more suitable to produce monolayers.

Further investigations on the phenotype of mTERT-MSC clarified that no effects on mTERT-MSC line phenotype are induced by the scaffold per se, independently of biological cues, throughout the culture time analyzed. When cultured for up to 6 days on all the matrices considered, mTERT-MSC continuously expressed the stemness phenotype, as demonstrated by the maintenance of Sca-1 antigen expression at high rate. Moreover, mTERT-MSC demonstrated the ability to differentiate towards the adipogenic and osteogenic phenotypes onto all the scaffolds tested. This evidence is in contrast with the recent findings by Engler and collaborators, who demonstrated that matrix elasticity is sufficient to direct mesenchymal stem cell fate within few days [19]. Such a discrepancy could reflect a divergent behavior between fresh and immortalized mesenchymal stem cells, but could also be explained by still unknown scaffold features.

Acknowledgments

References

[1] A. P. Beltrami, D. Cesselli, N. Bergamin, et al., "Multipotent cells can be generated in vitro from several adult human organs (heart, liver, and bone marrow)," *Blood*, vol. 110, no. 9, pp. 3438–3446, 2007.

[2] A. Gonzalez, M. Rota, D. Nurzynska, et al., "Activation of cardiac progenitor cells reverses the failing heart senescent phenotype and prolongs lifespan," *Circulation Research*, vol. 102, no. 5, pp. 597–606, 2008.

[3] L. G. Cima, J. P. Vacanti, C. Vacanti, D. Ingber, D. Mooney, and R. Langer, "Tissue engineering by cell transplantation using degradable polymer substrates," *Journal of Biomechanical Engineering*, vol. 113, no. 2, pp. 143–151, 1991.

[4] S. Cohen, M. C. Bano, L. G. Cima, et al., "Design of synthetic polymeric structures for cell transplantation and

tissue engineering," *Clinical Materials*, vol. 13, no. 1–4, pp. 3–10, 1993.

[5] G. Forte, F. Carotenuto, F. Pagliari, et al., "Criticality of the biological and physical stimuli array inducing resident cardiac stem cell determination," *Stem Cells*, vol. 26, no. 8, pp. 2093–2103, 2008.

[6] E. Fournier, C. Passirani, C. N. Montero-Menei, and J. P. Benoit, "Biocompatibility of implantable synthetic polymeric drug carriers: focus on brain biocompatibility," *Biomaterials*, vol. 24, no. 19, pp. 3311–3331, 2003.

[7] H. J. Kim, J. H. Lee, and G. I. Im, "Chondrogenesis using mesenchymal stem cells and PCL scaffolds," *Journal of Biomedical Materials Research Part A*. In press.

[8] N. J. Turner, C. M. Kielty, M. G. Walker, and A. E. Canfield, "A novel hyaluronan-based biomaterial (Hyaff-11®) as a scaffold for endothelial cells in tissue engineered vascular grafts," *Biomaterials*, vol. 25, no. 28, pp. 5955–5964, 2004.

[9] N. Landa, L. Miller, M. S. Feinberg, et al., "Effect of injectable alginate implant on cardiac remodeling and function after recent and old infarcts in rat," *Circulation*, vol. 117, no. 11, pp. 1388–1396, 2008.

[10] P. Bianco, M. Riminucci, S. Gronthos, and P. G. Robey, "Bone marrow stromal stem cells: nature, biology, and potential applications," *Stem Cells*, vol. 19, no. 3, pp. 180–192, 2001.

[11] G. Ferrari, G. Cusella-de Angelis, M. Coletta, et al., "Muscle regeneration by bone marrow-derived myogenic progenitors," *Science*, vol. 279, no. 5356, pp. 1528–1530, 1998.

[12] H.-F. Duan, C.-T. Wu, D.-L. Wu, et al., "Treatment of myocardial ischemia with bone marrow-derived mesenchymal stem cells overexpressing hepatocyte growth factor," *Molecular Therapy*, vol. 8, no. 3, pp. 467–474, 2003.

[13] A. J. Friedenstein, J. F. Gorskaja, and N. N. Kulagina, "Fibroblast precursors in normal and irradiated mouse hematopoietic organs," *Experimental Hematology*, vol. 4, no. 5, pp. 267–274, 1976.

[14] S. Nadri, M. Soleimani, R. H. Hosseni, M. Massumi, A. Atashi, and R. Izadpanah, "An efficient method for isolation of murine bone marrow mesenchymal stem cells," *International Journal of Developmental Biology*, vol. 51, no. 8, pp. 723–729, 2007.

[15] C. Holmes and W. L. Stanford, "Concise review: stem cell antigen-1: expression, function, and enigma," *Stem Cells*, vol. 25, no. 6, pp. 1339–1347, 2007.

[16] J. L. Simonsen, C. Rosada, N. Serakinci, et al., "Telomerase expression extends the proliferative life-span and maintains the osteogenic potential of human bone marrow stromal cells," *Nature Biotechnology*, vol. 20, no. 6, pp. 592–596, 2002.

[17] J. Yang, E. Chang, A. M. Cherry, et al., "Human endothelial cell life extension by telomerase expression," *The Journal of Biological Chemistry*, vol. 274, no. 37, pp. 26141–26148, 1999.

[18] X.-R. Jiang, G. Jimenez, E. Chang, et al., "Telomerase expression in human somatic cells does not induce changes associated with a transformed phenotype," *Nature Genetics*, vol. 21, no. 1, pp. 111–114, 1999.

[19] A. J. Engler, S. Sen, H. L. Sweeney, and D. E. Discher, "Matrix elasticity directs stem cell lineage specification," *Cell*, vol. 126, no. 4, pp. 677–689, 2006.

[20] K. Yoneno, S. Ohno, K. Tanimoto, et al., "Multidifferentiation potential of mesenchymal stem cells in three-dimensional collagen gel cultures," *Journal of Biomedical Materials Research Part A*, vol. 75, no. 3, pp. 733–741, 2005.

[21] W.-J. Li, R. Tuli, X. Huang, P. Laquerriere, and R. S. Tuan, "Multilineage differentiation of human mesenchymal stem cells in a three-dimensional nanofibrous scaffold," *Biomaterials*, vol. 26, no. 25, pp. 5158–5166, 2005.

[22] K. Stenderup, J. Justesen, C. Clausen, and M. Kassem, "Aging is associated with decreased maximal life span and accelerated senescence of bone marrow stromal cells," *Bone*, vol. 33, no. 6, pp. 919–926, 2003.

[23] M. K. Lee, M. P. Hande, and K. Sabapathy, "Ectopic mTERT expression in mouse embryonic stem cells does not affect differentiation but confers resistance to differentiation- and stress-induced p53-dependent apoptosis," *Journal of Cell Science*, vol. 118, no. 4, pp. 819–829, 2005.

[24] B. M. Abdallah, M. Haack-Sørensen, J. S. Burns, et al., "Maintenance of differentiation potential of human bone marrow mesenchymal stem cells immortalized by human telomerase reverse transcriptase gene despite of extensive proliferation," *Biochemical and Biophysical Research Communications*, vol. 326, no. 3, pp. 527–538, 2005.

[25] X. Zhang, Y. Soda, K. Takahashi, et al., "Successful immortalization of mesenchymal progenitor cells derived from human placenta and the differentiation abilities of immortalized cells," *Biochemical and Biophysical Research Communications*, vol. 351, no. 4, pp. 853–859, 2006.

[26] G. Huang, Q. Zheng, J. Sun, et al., "Stabilization of cellular properties and differentiation mutilpotential of human mesenchymal stem cells transduced with hTERT gene in a long-term culture," *Journal of Cellular Biochemistry*, vol. 103, no. 4, pp. 1256–1269, 2008.

[27] E. L. Herzog, L. Chai, and D. S. Krause, "Plasticity of marrow-derived stem cells," *Blood*, vol. 102, no. 10, pp. 3483–3493, 2003.

[28] S. S. Kang, T. Kwon, D. Y. Kwon, and S. I. Do, "Akt protein kinase enhances human telomerase activity through phosphorylation of telomerase reverse transcriptase subunit," *The Journal of Biological Chemistry*, vol. 274, no. 19, pp. 13085–13090, 1999.

[29] K. Liu, R. J. Hodes, and N.-P. Weng, "Cutting edge: telomerase activation in human T lymphocytes does not require increase in telomerase reverse transcriptase (hTERT) protein but is associated with hTERT phosphorylation and nuclear translocation," *The Journal of Immunology*, vol. 166, no. 8, pp. 4826–4830, 2001.

[30] M. Chen, P. K. Patra, S. B. Warner, and S. Bhowmick, "Role of fiber diameter in adhesion and proliferation of NIH 3T3 fibroblast on electrospun polycaprolactone scaffolds," *Tissue Engineering*, vol. 13, no. 3, pp. 579–587, 2007.